ISSN 1027-5495. Functional Materials, 22, No.1 (2015), p. 93-99.
doi:http://dx.doi.org/10.????/fm.220113

Influence of solution precursors on structure of ZnO films

T.O.Berestok, D.I.Kurbatov, N.M.Opanasyuk, A.S.Opanasyuk

Sumy State University, 2 Rimsky-Korsakov St., 40007 Sumy, Ukraine

Received September 22, 2014

In the work using high resolution scanning electron microscopy and X-ray analysis, we carry out the studying of the correlation between chemical and technological conditions of deposition, the initial solution composition and structural properties of the synthesized samples of zinc oxide. Growth of the layers depends on the initial precursors and it occurs through formation of the ordered array of nanorods and nanoflowers. It is shown that it is possible to choose the optimal conditions to obtain ZnO films with controlled structural properties that can be used as the base layers in microelectronic devices.

Keywords: ZnO nanorods, ZnO nanoflowers, chemical bath deposition, morphology, structure, sub-structure.

С использованием сканирующей электронной микроскопии и рентгеноструктурного анализа проведено определение взаимосвязи между физико-технологическими условиями осаждения, составом исходного раствора и структурными свойствами синтезированных образцов оксида цинка. Рост слоев зависит от начальных прекурсоров в исходном растворе и происходит путем формирования упорядоченного массива нановолокон или наноцветов. Выбраны оптимальные условия для получения пленок оксида цинка с контролируемыми структурными свойствами, которые могут быть использованы в качестве базовых слоев в микроэлектронике.

Вплив вихідних прекурсорів на структуру плівок ZnO. *Т.О.Берестoк, Д.І.Курбатов, Н.М.Опанасюк, А.С.Опанасюк*.

З використанням скануючої електронної мікроскопії та рентгеноструктурного аналізу проведено визначення взаємозв'язку між фізико-технологічними умовами осадження, складом вихідного розчину та структурними властивостями синтезованих зразків оксиду цинку. Ріст шарів залежить від початкових прекурсорів у вихідному розчині і відбувається шляхом формування упорядкованого масиву нановолокон або наноквітів. Обрано оптимальні умови для отримання плівок оксиду цинку з контрольованими структурними властивостями, які можуть бути використані як базові шари у мікроелектроніці.

1. Introduction

Owing to the wide range of zinc oxide applications as the base material of creation of gas sensors, sensors of various types of radiation, devices of micro- and optoelectronics, it was attracted a great attention of researchers [1]. Due to a large band gap $E_g = 3.37$ eV, ZnO can be used as window and conductive layers of solar cells [2]. In addition, the high carrier mobility and the possibility of obtaining of highly porous structures, zinc oxide can be used as a functional layer for creating sensitized solar cells of high efficiency based on perovskite absorbing layers [3]. High transparency in the visible region of the spectrum allows to use ZnO to create functional elements of transparent electronics [4].

Nowadays, for synthesis of zinc oxide films and nanostructures it can be used a large number of non-vacuum methods:

chemical vapor deposition [5], sol-gel method [6, 7], spray pyrolysis [8], hydrothermal synthesis [9–10], electrolytic deposition [11, 12, 13], chemical bath deposition from aqueous solution [14–18]. Last method is very promising due to its efficiency and simplicity. Also, it does not require maintenance of high temperature and pressure during the synthesis, which significantly reduces the cost of manufacturing of the device structures.

Synthesis of ZnO by low temperature no vacuum methods also makes it possible to obtain condensates on flexible substrates with controlled structural characteristics (such as nanodots, nanofibers, nano-porous and solid) which depend on the deposition conditions and source precursors [19, 20]. A number of works devoted to investigation of structural properties of zinc oxide films deposited by different methods [21, 22]. However structural and substructural characteristics of chemically deposited ZnO layers have been insufficiently studied. Therefore, the current work presents results of comprehensive study of the structural and substructural characteristics of two series of ZnO films samples, obtained by chemical bath deposition from solutions of zinc acetate and zinc nitrate. In addition, in the work we carried out the studying of the correlation between chemical and technological conditions of deposition, the composition of the initial solution on structural properties of the synthesized samples.

2. Experimental

Synthesis of two series of samples of zinc oxide condensates was performed by the method of chemical bath deposition under reactor temperature of 90°C. The films were obtained via dipping the substrates in solution of precursor's reagents. As precursors we used zinc salts: zinc acetate ($Zn(CH_3COO)_2 \cdot 2H_2O$) or zinc nitrate ($Zn(NO_3)_2$) with the chemical purity. To obtain solutions the distilled water was used. Initial concentration of the mixture was 0.1 M. To maintain pH of the solution about 10 the complexing agent — ammonia solution (NH_4OH) was added to it. As substrate we used glass and glass with FTO underlayer, which has been previously cleaned in acetone, isopropanol and ethanol and dried in nitrogen. Deposition time of the layers varied from $\tau = 30$ to 120 min with an interval of 15 minutes. After the films deposition the samples were dried under nitrogen and annealed in air at 350°C.

Investigation of morphology of the synthesized samples was performed using a scanning electron microscope ZEISS Avirguda. Structural investigations of the samples were performed using an automated X-ray diffractometer Bruker D8 Advance with Ni-filtered K_α — radiation of copper anode in a range of angles $20° < 2\theta < 80°$, where 2θ — the Bragg's angle. The diffraction patterns obtained under study were normalized to intensity of (002) peak of the hexagonal phase. X-ray radiation was focused according to the Bragg-Brentano method [23]. Processing of the diffractograms was carried out using of the Difwin software.

Phase analysis was performed by comparison of interplanar distances and relative intensities from the investigated samples and references according to the Joint Committee on Powder Diffraction Standards [24]. The curves were normalized to intensity of (002) peak of the hexagonal phase.

Texture quality of chalcogenide films was estimated using Harris method [23]. Pole density was calculated using equation:

$$P_i = \frac{(I_i / I_{0i})}{\frac{1}{N}\sum_{i=1}(I_i / I_{0i})},$$

where I_i, I_{0i} — integral intensity of the i-diffraction peak for the film samples and standards; N — number of lines in the diffraction pattern.

Thereafter we built the dependences $P_i - (hkl)_i$ and $P_i - \varphi$, where φ — angle between chosen direction and normal to different crystallographic planes, which correspond to reflection in the X-ray pattern, $(hkl)_i$ — Miller indices. This angle was calculated for the hexagonal lattice, using the equations given in [23]. The axis of the texture has indexes corresponding to the maximal value of P_i. Orientation factor was determined via equation $f = \sqrt{\frac{1}{N}\sum_{i=1}^{N}(P_i - 1)^2}$. Determination of the interplanar distances of wurtzite structure of ZnO was performed by position of $K_{\alpha 1}$ component of all of the most intense lines present in the XRD pattern.

Calculation of the lattice constants, a and c, of the hexagonal phase was held as:

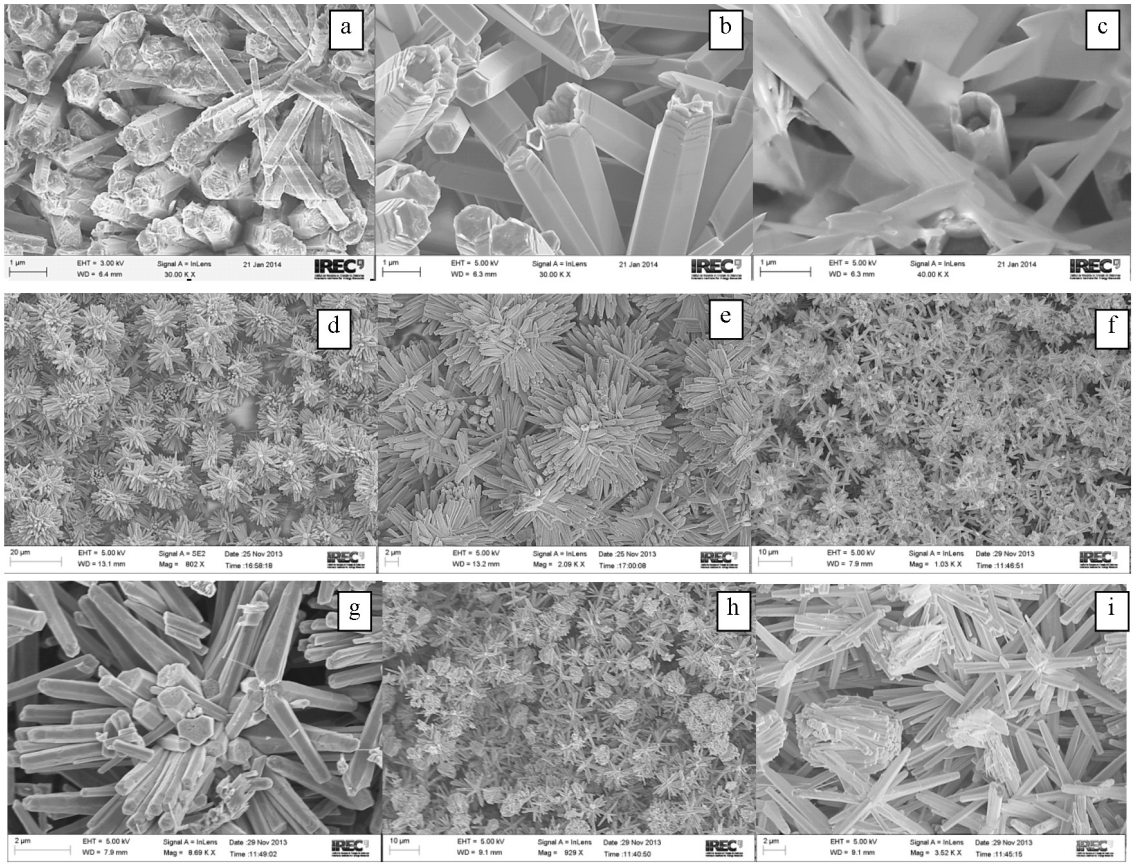

Fig. 1. Surface images of ZnO films deposited from solution of zinc nitrate after deposition time of τ = 60 min (a), 90 min (b), 120 min (c) and from solution of zinc acetate after deposition time of τ = 45 min (d, f), 90 min (g, e), 120 min (h, i).

$$a = \frac{\lambda}{2\sin\theta}\sqrt{\frac{4}{3}(h^2 + hk + k^2) + \left(\frac{a}{c}\right)^2 l^2}, \quad (1)$$

$$c = \frac{\lambda}{2\sin\theta}\sqrt{\frac{4}{3}\left(\frac{c}{a}\right)^2(h^2 + hk + k^2) + l^2}, \quad (2)$$

where λ — is a wavelength of X-rays.

The ratio c/a was considered as a constant and equal to the value of the wurtzite structure of ideal lattice $c/a = 1.601$ [24].

Further the values of the lattice constants of ZnO were clarified using the Nelson-Riley extrapolation method [25]. At the same time we used graphical method of successive approximations, which included an iterative procedure. From dependences $a(c) - 1/2\cos^2\theta(1/\sin\theta + 1/\theta)$ we determined values of the lattice parameters, a and c, and the ratio c/a. Calculated ratio c/a (a/c) was used to estimate new constants from equations (1) and (2). Thereafter the iterative procedure was repeated several times (up to four), while the obtained values, a, c and c/a, converged [23]. An approximation of the points in $a(c) - 1/2\cos^2\theta(1/\sin\theta + 1/\theta)$ dependences was made with the help of the least-squares method using the OriginPro software package. The proposed procedure of determining the lattice parameters (a, c) allowed to significantly increase the accuracy of measurements. The values of a, c obtained after fourth iteration were used to calculate the volume of hexagonal primitive cell using expression $V = (3\sqrt{3}a^2c)/2$.

Traditionally, determining of grain size is performed by electron microscopy using the Scherrer equation [18, 21, 22]. Despite that we used diffractometrical method in order to estimate the average size of coherent scattering domain size (CSD) L and level of microstrain (ε) by the half-width of the diffraction lines. To separate the diffraction broadening caused by physical and instrumental effects we used approximations of X-ray line by the Cauchy and Gauss functions. Further separation of contributions from dispersion on CSD and microstrain was performed by the graphical Williamson-Hall method. Accordingly it was built the

graphics in coordinates $\beta\cos\theta/\lambda - (4\sin\theta/\lambda$ and $(\beta\cos\theta/\lambda)^2 - (4\sin\theta/\lambda)^2$, where β — is physical broadening of X-ray line [19]. Additionally microstrain and size of CSD were determined by the method of approximation with present of X-ray line as a threefold convolution [23, 25]:

$$L = \frac{\lambda}{\cos\theta_1} \cdot \frac{tB_1 - cB_2}{t\beta_{f1}^2 - \beta_{f2}^2}, \quad (3)$$

$$\varepsilon^2 = \frac{c\beta_{f1}^2 B_2 - \beta_{f2}^2 B_1}{16\mathrm{tg}\theta_1 (cB_2 - tB_1)}, \quad (4)$$

where $t = \mathrm{tg}^2\theta_2/\mathrm{tg}^2\theta_1$; $c = \cos\theta_1/\cos\theta_2$; $\beta_{fi} = \sqrt{(B_i)^2 - (b_i)^2}$; θ_1 and θ_2 — are diffraction angles of the pairs of analyzed lines; B_i, b_i, β_{fi} — measured, instrumental and physical broadening of the corresponding X-ray lines.

3. Results and discussion

Surface images of the condensates deposited during different deposition time are shown in Fig. 1. Studies have shown that during the deposition from solution of zinc nitrate, the condensates had poor adhesion to the glass substrate surface. Growth of zinc oxide films occurred through formation of an ordered array of hexagonal nanorods (Fig. 1a) with thickness (0.2–0.8 μm) and length (2.0–3.5 μm). Furthermore obtained nanorods had different angles to the substrate (τ = 60 min). With increasing duration of deposition to 90 min. (Fig. 1b), there was an increase in both, thickness (1.0–1.9 μm) and length (4.8–6.7 μm) of the nanorods. Increasing of the deposition time to 120 min led to the merging gaps between the nanorods by lamellar crystallites with thickness 0.10–0.16 μm. And therefore it led to the formation of a continuous film (Fig. 1c).

After the deposition of the condensates onto glass substrates with FTO underlayer from zinc acetate solution (τ = 45 min), there was a formation of nanoflowers of ZnO. They consisted of outlets of the nanorods with hexagonal shape (length 3.7–4.4 μm and thickness of 0.5–0.6 μm) oriented at different angles to the substrate. Additionally, the nanorods were slightly narrowed to its end (Fig. 1c, d).

With increasing of deposition time to 90 min, there took place the growth of the nanoflowers next layer on the first one

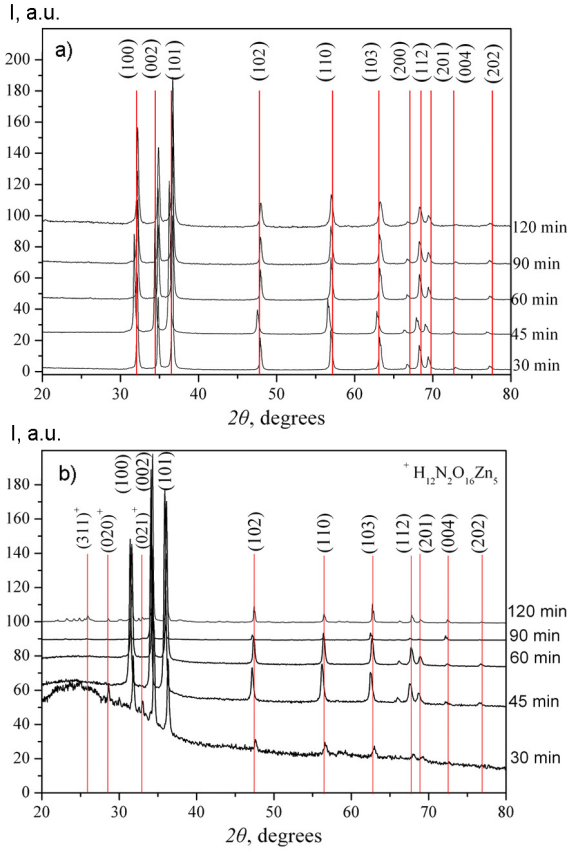

Fig. 2. XRD patterns of the films obtained from zinc acetate (a) and zinc nitrate (b) solutions after different duration of deposition.

(Fig. 1g, e). Furthermore the size of the nanorods, which formed flowers, slightly increased. As it can be seen from Fig. 1e, the nanorods were porous. After extending of duration of the deposition to 120 min, with formation of the new nanoflowers, there was a growth of the nanorods bundles, approximately, same length (6.3–7.5 μm) and thickness (0.6–0.7 μm) (Fig. 1h, i).

As a result, growth of the labyrinthine structure with high surface area to the substrates was occurred onto substrates. It should be noted that despite its tracery, layers have high adhesion to the substrate's surface. In case of using of zinc acetate as precursor, the nanorod's surface was smoother than in the case of zinc nitrate using.

Phase analysis showed (Fig. 2a) that the samples of zinc oxide obtained from solution of zinc acetate were single phase in whole range of the deposition time (τ = 30–120 min). And in the XRD pattern, the lines at the angles of 36.65°, 34.83°, 32.16° were with dominant intensity. They were identified as reflection of the crystal-

lographic planes (101), (002) and (100) of hexagonal phase of ZnO, respectively. In addition, there were also registered the reflections from crystallographic planes of (102), (110), (103) at the angles of 47.93°, 56.94°, 63.19°.

X-ray patterns from zinc oxide layers synthesized from zinc nitrate solution were presented in Fig. 2b. Phase analysis showed that in the spectra the maximal intensity had reflections from crystallographic planes (002) of hexagonal phase of ZnO. Also in the diffractograms we registered fairly intense lines at the angles of 31.65°, 36.13°, 47.52°, that we identified as a reflection of the planes (100), (101), (102) of wurtzite phase of zinc oxide, respectively [24].

In addition in the diffractograms of ZnO layers of small thickness (deposition duration <90 min) there were present extraneous peaks at the angles of 26.03°, 28.72°, 32.99°, which were identified as reflections from planes of (311), (020), (021) of $H_{12}N_2O_{16}Zn_5$ [24]. Presence of extraneous phase may be due to incorporation in the crystal structure of the condensation products of residual sediment during the chemical reaction.

It should be noted that the presence of extraneous phases was not observed in the samples obtained from zinc acetate solution as source precursor and annealed in air at 350°C.

Results of the calculation of reverse pole figures (Fig. 3a, b) showed that the samples of zinc oxide deposited from zinc nitrate solution have high (f = 0.45–1.83) growth texture of [002] (Fig. 3a, inset). While the samples synthesized using zinc acetate as a source precursor had worse quality of growth texture of [002] (f = 0.16–0.27) (Fig. 3b, inset). These findings are supported by electron microscopic images of the samples surface. Furthermore quality of textures depended on the duration of deposition with slightly varying in the both cases. It should be noted, that growth texture [002] is typical when zinc oxide films are synthesized by chemical bath deposition from the solutions of zinc nitrate and ammonia [16], and zinc acetate and ammonia [18].

Table shows the results of the precision determination of the lattice constants of synthesized ZnO samples. We showed the data obtained after the fourth iteration, because the values of a, c and their ratio c/a were practically unchanged after fourth iteration, indicating about finishing of calculation procedure. It was found that the lattice constants of ZnO layers, deposited from the solution of zinc acetate, were in the range of a = 0.32488–0.32548 nm, c = 0.52010–0.52083 nm; lattice parameters of the condensates deposited from the solution of zinc nitrate were equal to a = 0.32486–0.32548 nm, c = 0.52064–0.52149 nm. The analysis showed that obtained values of a were slightly lower than the reference one (a = 0.3256 nm); while the values of c were close to the reference for the solid material (c = 0.5212 nm). The result of the parameters a and c calculations allowed to determine their ratio and volume of the lattice cell of ZnO (Table). It was found that increasing of deposition time of the films obtained from a solution of zinc nitrate led to decrease of c/a ratio from 1.6034 to 1.5996, with following increasing to 1.6027. A similar tendency was observed for samples deposited from the solution of zinc acetate. Volume of the lattice cell of the material was equal to $V = (0.1428–0.1434)\cdot10^{-27}$ m^3.

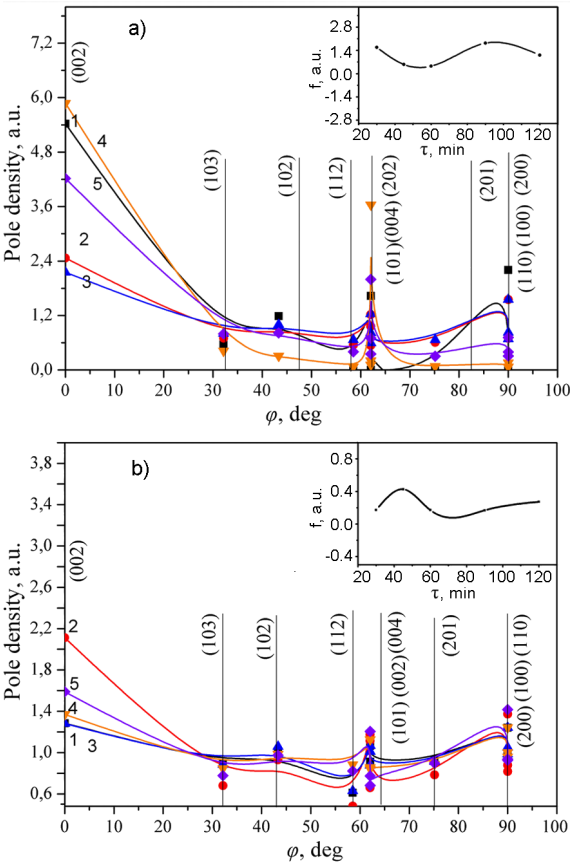

Fig. 3. Dependencies of pole density and orientation factor (inset) on deposition time of condensates deposited from zinc nitrate (a) and zinc acetate (b): *1* — τ = 30 min, *2* — 45 min, *3* — 60 min, *4* — 90 min, *5* — 120 min.

Table. Calculation of the lattice parameters of ZnO condensates

τ, min	ZnO							
	Zinc acetate				Zinc nitrate			
	a, nm	c, nm	c/a	$V\cdot10^{27}$, m^3	a, nm	c, nm	c/a	$V\cdot10^{27}$, m^3,
30	0.32514	0.52082	1.6018	0,1430	0.32486	0.52087	1.6034	0.1428
45	0.32536	0.52115	1.6018	0,1433	0.32534	0.52096	1.6013	0.1432
60	0.32548	0.52064	1.5996	0,1432	0.32548	0.52064	1.5996	0.1433
90	0.32523	0.52010	1.5992	0,1429	0.32538	0.52145	1.6026	0.1434
120	0.32488	0.52083	1.6031	0,1428	0.32538	0.52149	1.6027	0.1434
[22]	a = 0.3256 nm, c = 0.5212 nm, c/a = 1.601, V = 0.1435·10^{-27} m^3							

These values were lower in the following directory for massive material (V = 0.1435·10^{-27} m^3).

Dependences of CSD size $L_{(002)}$ and level of microstrain $\varepsilon_{(002)}$ in the direction perpendicular to the atomic planes (002) on the duration of deposition are shown in Fig. 4. As it was mentioned above, the results were obtained using three different approximations described in methods.

Because values of the substructural parameters of ZnO determined from threefold convolution were the most accurate and close to the real ones; thus we discussed the results based on it. Calculation of the substructure of synthesized films showed that the average size of CSD in the condensates deposited from zinc nitrate solution decreased with increasing of the deposition time from $L_{(002)}$ = 42 nm (τ ~ 30 min) to $L_{(002)}$ = 26 nm (τ ~ 120 min) (see Fig. 4a). For ZnO samples synthesized from zinc nitrate solution, we observed a reverse trend: increasing deposition time led to increase of CSD size from 29 nm to 33 nm (Fig. 4b). The authors of [22] obtained slightly larger values of CSD (L = 55±11 nm) using the Scherrer equation for electrodeposited ZnO films. Level of microstrain (Fig. 4a, inset) in ZnO condensates deposited from zinc nitrate solution, decreased monotonically with increasing of deposition time τ from ε ~ 3.09·10^{-3} to ε ~ 0.59·10^{-3}. In ZnO condensates obtained from zinc acetate solution, values of microstrains (Fig. 4b, inset) increased with increasing deposition time τ from ε ~ 1.2·10^{-3} to ε ~ 2.12·10^{-3}. At the same time these values were lower than in the samples obtained from the solution of zinc nitrate.

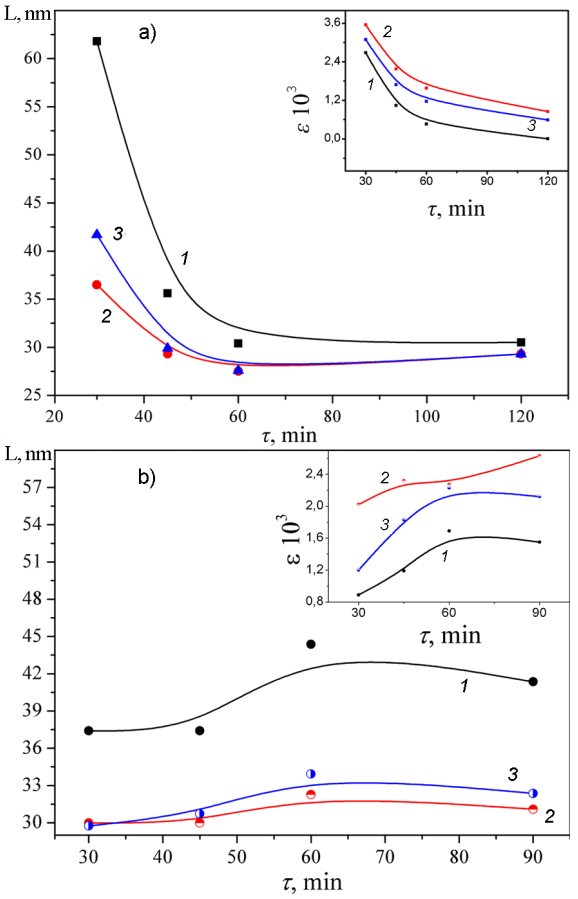

Fig. 4. Dependences of CSD size L and microstrain in crystallographic direction (002) on deposition time for the samples of ZnO obtained from zinc nitrate (a) and zinc acetate (b). Approximation by the Gauss (*1*) and Cauchy (*2*), threefold convolution method (*3*).

4. Conclusions

In this paper we investigated an influence of precursor composition on the structural and substructural characteristics of zinc oxide condensates synthesized by chemical bath deposition from zinc nitrate

and zinc acetate solutions at different deposition duration. It was established that ZnO films, deposited from zinc nitrate solution, had poor adhesion to the surface of the glass substrate; and the growth of the layers occurred through the formation of an ordered array of nanorods. The growth of condensates deposited on FTO substrate from zinc acetate solution occurred through formation of ZnO nanoflowers with the high specific surface area. This layer had a high adhesion to the substrate surface.

It was found that the samples synthesized from zinc acetate solution after annealing at 350°C were single phase with stable hexagonal structure. Despite that, there were registered the presence of extraneous phase in ZnO films with low thickness, deposited from zinc nitrate solution. ZnO films obtained from the both solutions showed the growth texture of [002]. At the same time, the layers obtained from zinc nitrate solution had higher quality of growth texture ($f = 0.45–1.83$) compared with the samples deposited using zinc acetate as an initial precursor ($f = 0.16–0.27$).

Precision values of the lattice parameters of the material ($a = 0.32486$ nm, $c = 0.52087$ nm — for condensates deposited from zinc nitrate solution; $a = 0.32514$ nm, $c = 0.5208$ nm — deposited from zinc acetate solution) showed that these values were well correlate with reference one ($a = 0.3256$ nm, $c = 0.5212$ nm).

It was shown that the average size of CSD in the condensates deposited from zinc nitrate solution, decreased with increasingof deposition time from $L_{(002)} = 42$ nm ($\tau \sim 30$ min) to $L_{(002)} = 26$ nm ($\tau \sim 120$ min), while for ZnO samples synthesized from zinc nitrate solution, there was observed the inverse trend: CSD size increased from 29 nm to 33 nm with increasing deposition time. Level of microstrain of ZnO condensates deposited from zinc nitrate solution decreased monotonically with increasing deposition time τ from $\varepsilon \sim 3.09 \cdot 10^{-3}$ to $\varepsilon \sim 0.59 \cdot 10^{-3}$. In ZnO condensates obtained from zinc acetate solution, microstrain increased with increasing deposition time τ from $\varepsilon \sim 1.2 \cdot 10^{-3}$ to $\varepsilon \sim 2.12 \cdot 10^{-3}$.

With the help of this research we can choose the optimal conditions to obtain ZnO films with controlled structural properties that can be used as the base layers in microelectronic devices.

References

1. J.Guo, J.Zhang, M.Zhu et al., *Sensor.Actuat. B-Chem*, **199**, 339 (2014).
2. R.Scheer, H.-W.Schock, Chalcogenide Photovoltaics: Physics, Technologies, and Thin Film Devices, WILEY-VCH Verlag GmbH & Co. KGaA (2011).
3. M.H.Kumar, N.Yantara, S.Dharani et al., *Chem. Commun.*, **49**, 11089 (2013),
4. R.Triboulet, *Prog. Cryst. Growth Ch.*, **60**, 1 (2014).
5. Y.Kashiwaba, F.Katahira, K.Haga et al., *J. Cryst. Growth*, **221**, 431 (2000).
6. C.Amutha, A.Dhanalakshmi, B.Lawrence et al., *Progr. Nanotechn. Nanomater.*, **3**, 13 (2014).
7. A.D.Pogrebnjak, A.A.Muhammed, E.T.Karash et al., *Prz. Elektrotechniczn.*, **3b**, 315 (2013).
8. A.Gahtar, A.Rahal, B.Benhaoua, S.Benramache, *Optik — Intern. J. Light and Electron Optics*, **125**, 3674 (2014).
9. J.Fan, Y.Hao, C.Munuera et al., *J. Phys. Chem. C*, **117**, 16349 (2013).
10. J.Fan, Y.Hao, A.Cabot et al., *ACS Appl. Mater.& Interfaces*, **5**, 1902 (2013).
11. J.D.Fan, C.Fabrega, R.Zamani et al., *J. Alloys Compd.*, **555**, 213 (2013).
12. J.Fan, R.Zamani, C.Fabrega et al., *J. Phys. D: Appl. Phys.*, **45**, 415301 (2012).
13. J.Fan, F.Guell, C.Fabrega et al., *J. Phys. Chem. C*, **116**, 19496 (2012).
14. S.B.Jambure, S.J.Patil, A.R.Deshpande, C.D.Lokhande, *Mater. Res. Bull.*, **49**, 420 (2014).
15. K.V.Gurav, U.M.Patil, S.M.Pawar et al., *J. Alloys Compd.*, **509**, 7723 (2011).
16. Q.Li, J.Bian, J.Sun et al., *Appl. Surf. Sci.*, **2561**, 698 (2010).
17. R.Saravana Kumar, R.Sathyamoorthy, P.Matheswaran et al., *J. Alloys Compd.*, **506**, 351 (2010).
18. H.-C.Cheng, C.-F.Chen, C.-Y.Tsay, J.-P.Leu, *J. Alloys Compd.*, **475**, L46 (2009).
19. T.O.Berestok, D.I.Kurbatov, N.M.Opanasyuk et al., *J. Nano-Electron. Phys.*, **5**, 01001(2013).
20. A.S.Opanasyuk, T.O.Berestok, P.M.Fochuk et al., *Proc. of SPIE*, **8823**, 88230Q1 (2013).
21. W.-J.Lee, J.-G.Chang, S.-P.Ju et al., *Nanoscale Res. Lett.*, **6**, 352 (2011).
22. T.Mahalingam, V.S.John, L.S.Hsu, *J. New Mat. Electrochem. Syst.*, **10**, 9 (2007).
23. Ja.S.Umanskij, Ju.A.Skakov, A.N.Ivanov, L.N.Rastorgujev, Crystallogaphy, X-ray Graph and Electronmicroscopy, Metallurgy, Moscow (1982) [in Russian].
24. Selected Powder Diffraction Data for Education Straining (Search Manual and Data Cards), Published by the International Centre for Diffraction Data, 432 (1997).
25. V.V.Kosyak, D.I.Kurbatov, M.M.Kolesnyk et al., *Mater. Chem. Phys.*, **138**, 731 (2013).